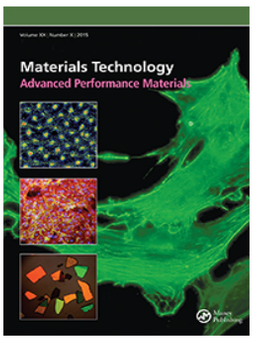

Taylor & Francis
Taylor & Francis Group

Materials Technology
Advanced Performance Materials

ISSN: 1066-7857 (Print) 1753-5557 (Online) Journal homepage: https://www.tandfonline.com/loi/ymte20

High-performance all-optical switching based on nonlinear response in semiconductor $Bi_2S_{3-x}Se_x$/PMMA nanocomposite films

M.Y. Shubar, H.L. Saadon & Saeed J. Abbas

To cite this article: M.Y. Shubar, H.L. Saadon & Saeed J. Abbas (2019): High-performance all-optical switching based on nonlinear response in semiconductor $Bi_2S_{3-x}Se_x$/PMMA nanocomposite films, Materials Technology, DOI: 10.1080/10667857.2019.1701253

To link to this article: https://doi.org/10.1080/10667857.2019.1701253

Published online: 11 Dec 2019.

Submit your article to this journal

Article views: 18

View related articles

View Crossmark data

Full Terms & Conditions of access and use can be found at
https://www.tandfonline.com/action/journalInformation?journalCode=ymte20

MATERIALS TECHNOLOGY
https://doi.org/10.1080/10667857.2019.1701253

Taylor & Francis
Taylor & Francis Group

Check for updates

High-performance all-optical switching based on nonlinear response in semiconductor $Bi_2S_{3-x}Se_x$/PMMA nanocomposite films

M.Y. Shubar, H.L. Saadon and Saeed J. Abbas

Laser Applications Research Group (LARG), Department of Physics, College of Science, University of Basrah, Basrah, Iraq

ABSTRACT

We present an optical pump-probe technique to optimise the all-optical photonic switching based on $Bi_2S_{3-x}Se_x$/PMMA nanocomposite films. $Bi_2S_{3-x}Se_x$/PMMA nanocomposite films were prepared using a microwave-assisted synthesis with different compositions of x. Crystal structure, surface morphology, and optical properties were performed to characterise the prepared nanocomposite films. The crystallinity and optical band gap of the prepared $Bi_2S_{3-x}Se_x$/PMMA were affected by x. The prepared samples showed a blue shift in the absorption edge. The optical nonlinearity of the films exhibited switchover from self-defocusing to focusing effect, and saturable absorption to reverse saturable absorption, investigated using the Z-scan technique. The all-optical switching performance of the $Bi_2S_{3-x}Se_x$/PMMA nanocomposite films under different compositions x was investigated. The results showed that the $Bi_2S_{3-x}Se_x$ /PMMA at x = 0.4 and 1.0 can demonstrate an all-optical switching at threshold pump power of 13 mW and lead to the realisation with maximum modulation depth of 76% and 80% with minimum switching contrast of 6.2 dB and 7 dB at switching time of 14 ms and 13 ms, respectively.

ARTICLE HISTORY
Received 9 July 2019
Accepted 28 November 2019

KEYWORDS
All-optical switching; bismuth chalcogenides; $Bi_2S_{3-x}Se_x$/PMMA nanocomposite; modulation depth; switching contrast

Introduction

All-optical switching is essential optical components of photonic networks and can control of incident light by using nonlinear optical (NLO) material and not by an electrical or a mechanical control which are highly desirable and interest for the time being. Therefore, all-optical switching can perform the function of control light-induced cutting-off of the signal light, i.e. it possesses the ON/OFF conversion function. Hence, all-optical switching can be regarded as a core element, playing a crucial and essential role in constructing on-chip all-optical switch networks [1,2]. The ability of light to control the reflection, refraction, or transmission of the beam of light itself or other beams in a material depends on the nonlinear optical responses of the material and their type of nonlinearity. Materials with good optical nonlinearities need to be developed in order to realise the full potential of such optical devices. As digital information continues to develop quickly, the light dependent-based technologies were seemed increasing attention from researchers in recent years [3–5]. After the coming of laser, photonic crystals have made a significant role in information technology [6,7] over 30 years ago. The continuous integration of the light into all-optical information or devices and emerging optical technologies appeals the ability to control light by design. Alternatively, control and manipulation of light in all-optical switching could be achieved by directly using the optical nonlinearity of materials [8,9]. In this regard, all-optical switches are devices used in all-optical communication and computer network that can establish the connection of optical signals [10], which that abruptly turns zero transmission above a certain threshold intensity. The all-optical switching property is closely related to the material of the device.

Until now, many materials for optical switching devices have been reported, including inorganic, semiconductor materials, organic, and hybrid materials between organic-inorganic compounds [11,12] and so on. In addition to, low dimensional materials (such as 0D, 1D and 2D) included into these materials also, because their properties can be tuned by changing their shapes and sizes. Many authors have been investigated nonlinear optical effects in such materials, for example, refs [12–14]. They used few layers of antimonene-based, bismuthine-coated microfiber and phosphorene-decorated microfiber as all-optical processing and other applications. However, optical devices based on nanocomposite materials containing semiconductors in a polymer matrix have been little reported. Recently, we have reported the all-optical switching of metal-doped PbS/PVA freestanding nanocomposite films [8]. The composed semiconductors with polymers added many benefits to resulting materials, since the new material will inherit the properties of the parent material and give researchers abilities to tuning their properties as they wanted.

CONTACT H.L. Saadon haithamsaadon@yahoo.com Laser Applications Research Group (LARG), Department of Physics, College of Science, University of Basrah, Basrah, Iraq

© 2019 Informa UK Limited, trading as Taylor & Francis Group

There are many technologies can be used in light controlling with light, one of them by using nonlinear optical materials. The basic principle of this device may be depended on the variation of nonlinear refractive index, single-photon absorption, two-photon absorption or multiphoton absorption. Another approach is by the use of the nanoscale optical waveguide and nanomaterial (photonic crystal and surface plasmon polariton). By using various nano-structures and new physical mechanisms compress the device space dimension and the pulse width of driving laser and in the same time to enhance the nonlinearity, response time and transparency of material

In this paper, the all-optical switching has been investigated of $Bi_2S_{3-x}Se_x$/PMMA nanocomposite films in different compositions of x and determined their nonlinear optical responses by a modified z-scan technique under a green pump laser beam at a wavelength of 532 nm. The obtained results have led to the building up of an all-optical switching device with enhanced parameters (modulation depth MD, switching contrast SC, and switching time ST) related to the composition x in the $Bi_2S_{3-x}Se_x$/PMMA nanocomposite films.

Materials and preparation samples

Materials

Bismuth Chloride (Reagent grade, 98%), Thiourea (Alfa, 99%), Ethylene Glycol (Riedel-de Haen, 99%), Telluride (Fluka, 99%), Chloroform (Scharlau, synthesis grade stabilised with ethanol), Sodium selenite (CDH Analytical Reagent, 99%) and Poly (methyl methacrylate) powder (Reagent grade, 97%) were used. All chemicals were used as received without any further treatments.

Preparation of the bismuth chalcogenides

Bismuth chalcogenides (S, Se) are prepared by the microwave-assisted synthesis. The representative scheme of the method is illustrated in Figure 1. First, the source of bismuth ($BiCl_3$ = 0.4 M) is dissolved carefully in 12.5 ml of EG with helping of the magnetic stirring. Secondly, the source of chalcogen anion (S or Se to S ratio) is added to the solution of the bismuth with conduction of continuous stirring. Here, we have studied the effect of change of the mole fraction of Se with respect to S on the properties of the ternary compound ($Bi_2S_{3-x}Se_x$, x = 0.0, 0.2, 0.4, and 1.0). Finally, the mixed solution is exposed to microwave radiation. To avoid the excess pressure generating by heat, we used an open reactor with on/off time of the microwave power equal to 10 s/20 s for 2 min. The microwave power is provided from a commercial microwave oven with a radiated power 720 W. the black precipitate is filtered by a filter paper and washing for several times by the distilled water and ethanol to remove any unreacted materials. Then, the filtrate is left in a petri dish at 60°C for 2 h to dry.

Preparation of $Bi_2S_{3-x}Se_x$/pmma nanocomposite films

The lack of the bismuth semiconductor compounds to solution processing was to make it as a thin film for the practical application. We composed it with polymer PMMA, which has good optical and mechanical properties, as well as it is has a good solubility in the many popular solvents.

To prepare a nanocomposite film of $Bi_2S_{3-x}Se_x$/PMMA, where x = 0.0, 0.2, 0.4, 1.0, we wanted to point out that thorough all this article, here x refers to the molar ratio between sodium selenite to the Thiourea in the solution, which means the ratio of Se to S). We are thoroughly mixing of the same amount of the semiconductor and the PMMA polymer (0.02 g of each) in 5 ml of the chloroform under vigorous magnetic stirring for 1 h. The films are deposited on glass substrates and left to dry naturally at the room temperature. The obtaining films

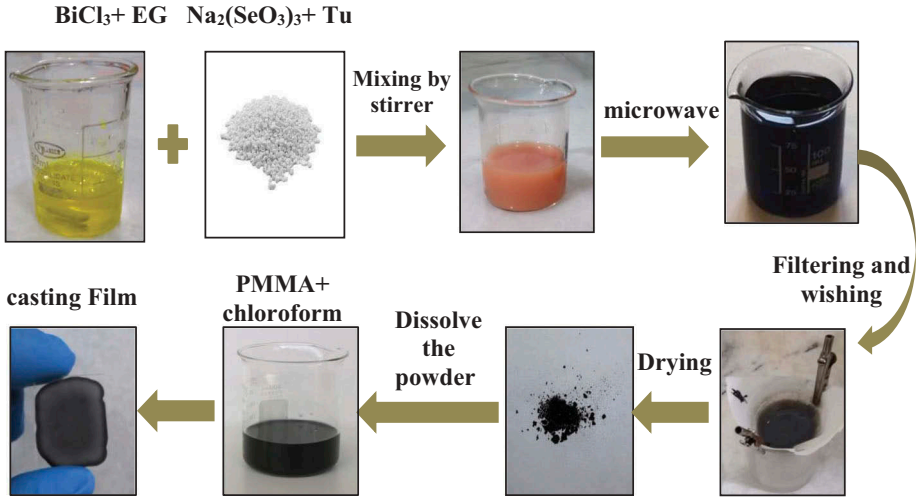

Figure 1. Schematic steps of the sample preparation process.

have uniform surface and their thickness approximately with the range (105 ± 10) μm.

Characterisation techniques

The x-ray diffraction (XRD) pattern is investigated by using PANalytical X'PertPRO with CuKα (wavelength of λ = 1.5406 Å) from Philips company. The morphology is observed by Scanning electron microscope (SEM, NOVA NAAOSEM 450) with energy dispersive X-ray (EDX) unit attached with it for inspection of the elemental composition. Optical absorption is measured by using a UV-Vis spectrophotometer type (UV-1800 SHIMADZU) in the wavelength range from 300 to 900 nm.

Experimental technique and its principle

In principle, all-optical switching can modulate the probe (or signal) light propagation through a control (or pump) light, realised using various optical nonlinear effects. In practical, all-optical switching devices can be constructed using photonic micro/nano-structures as a matrix, containing nonlinear optical materials. All-optical switching is based on all-optical mechanisms and depends on NLO materials that exhibit one or more of the nonlinear optical mechanisms: nonlinear refraction and nonlinear absorption [15–18]. After excitation by a pump laser beam, the material exhibits changes in the atomic or molecular structure through the change in the nonlinear optical properties (nonlinear absorption or nonlinear refraction).

In this context, the optical pump-probe technique was presented for characterisation of the all-optical switching effect. This technique is based on a single-input pump polarisation state to pump the NLO material simultaneously and is illustrated in Figure 2. The diode-pumped solid-state laser with transistor–transistor logic operating at 532 nm in the TEM_{00} mode was used as the pump beam modulated at different frequencies. A He-Ne CW laser at 632.8 nm was used as the probe beam. The sample was placed between two crossed polarisers P1 and P2. A linear polariser was added to the pumping beam. The angle between the polarisation directions of the polariser P3 was fixed at an angle of 45° with respect to the polarised direction of P1. The optical change in the sample was induced by the pump beam and monitored by the detection of the transmitted intensity through the polariser P3. The transmitted intensity was automatically recorded by a computer with a digital oscilloscope.

Results and discussion

Crystalline structure

The XRD patterns of the $Bi_2S_{3-x}Se_x$ at different compositions, x = 0.0, 0.2, 0.4, and 1.0 are shown in Figure 3. All the diffraction peaks are labelled and can be indexed to an orthorhombic structure. All patterns

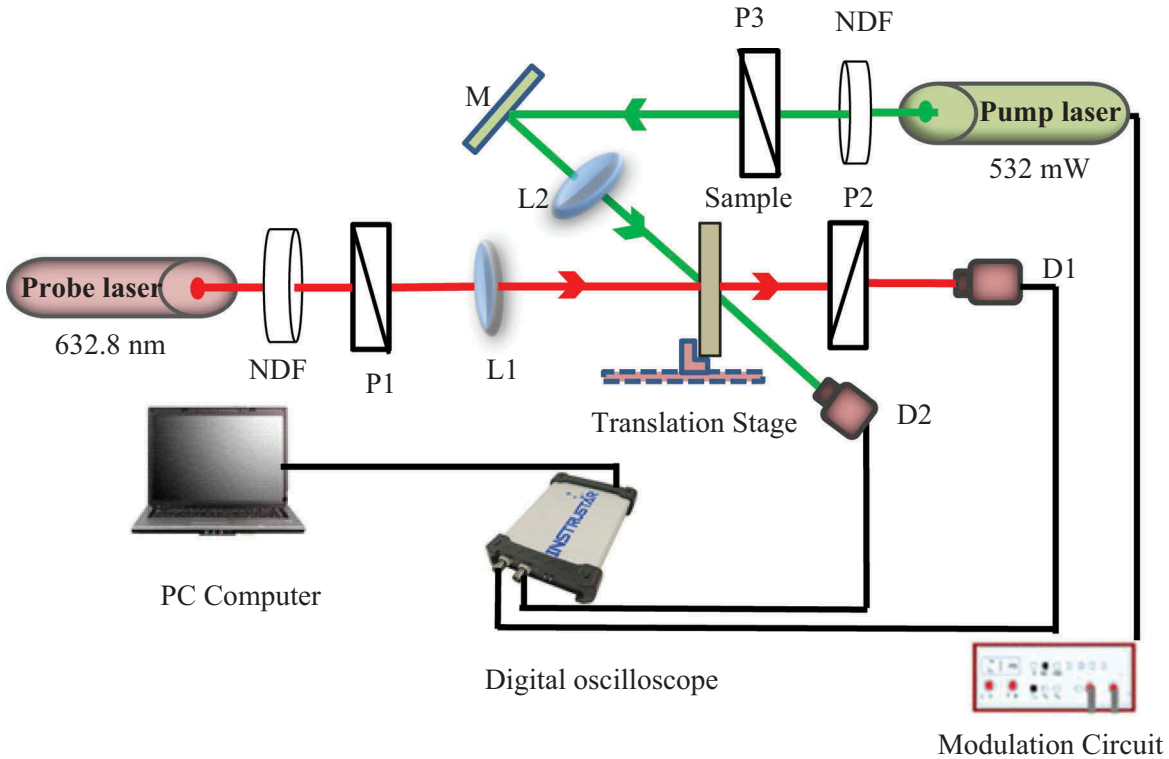

Figure 2. Optical pump-probe technique for investigating of all-optical switching in $Bi_2S_{3-x}Se_x$/PMMA films. P1, P2, and P3 are polarisers; NDF: Neutral density filter; F: Optical filter; D1 and D2 are detectors; L1 and L2 convex lens; and M is mirror.

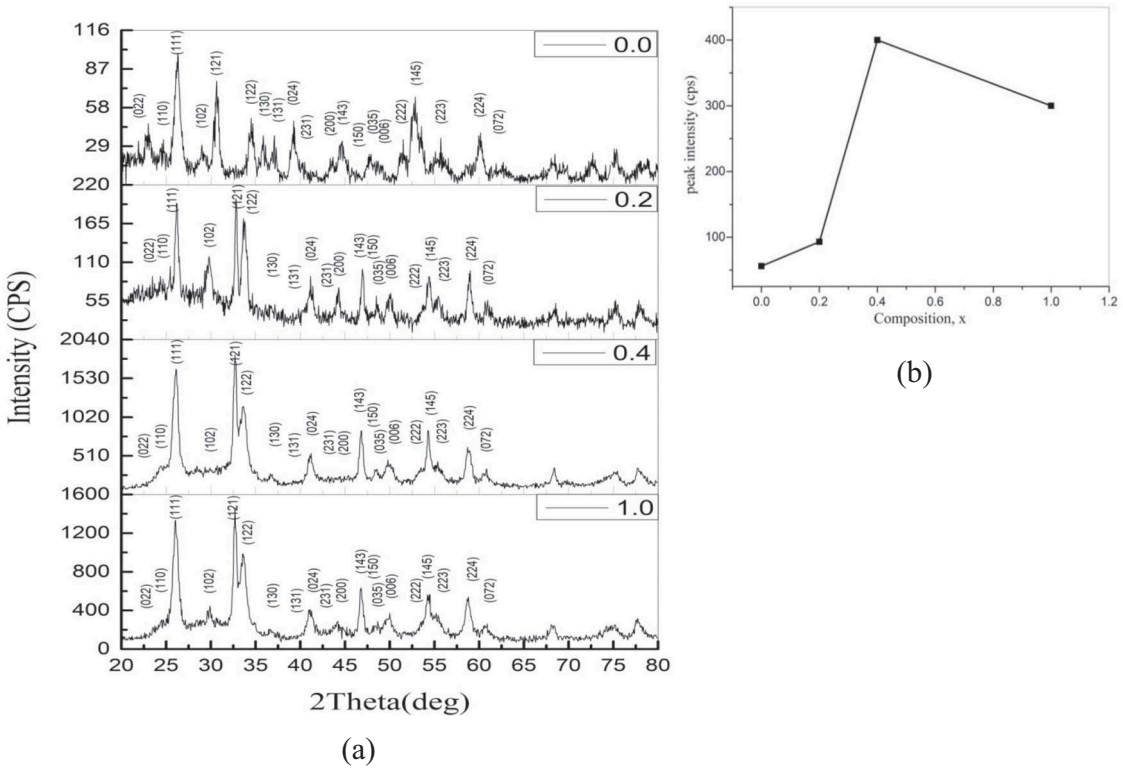

Figure 3. (a) X-ray diffraction patterns of $Bi_2S_{3-x}Se_x$/PMMA nanocomposite films at different compositions, x = 0.0, 0.2, 0.4, and 1.0. (b) The peak intensity as a function of x composition.

(i.e. for all Se to S ratio) exhibit the same crystal structure as the binary Bi_2S_3 (i.e. x = 0.0). The lattice constants are a = 11.22 Å, b = 10.9 Å, and c = 4.03 Å; these values are at well agreement with standard reported (JCPDS No. 170,320) [19]. All main peaks are the same in each pattern, but there is a small shift due to the difference of the atomic radius of Se and S atoms [20], and replacing the S with Se makes no change in crystal structures. Here, a systematic shift of the most intense XRD peaks for the (122) plane was observed [20], as well as high crystallisation peaks for the (122) plane and low crystallisation in (131) and (130) planes. The XRD peak intensity increased when the Se:S ratio reaches to 0.4 M, indicating the enhanced crystallinity of prepared nanocomposites. At Se:S = 1.0 M, there was a decrease in the crystallinity as shown in Figure 3(b); similar result has been reported of other nanocomposite materials [8,21].

SEM and EDX studies

The surface morphology (SEM images) of the $Bi_2S_{3-x}Se_x$ is shown in Figure 4 at different compositions of x. The SEM images appeared, there are two kinds of nanostructures. One is a nanowire and the other is nanosheets. It can be revealed that the prepared samples have good surface morphology and quality. As shown in the figure, the Bi_2S_3 nanowires have an average length of 1640 nm and a width of 47.3 nm. The ternary $Bi_2S_{3-x}Se_x$ sample has an average length equal to 241.4 nm with a width of 56.72 nm. The formation of nanowires at x = 0.0 and 0.4, which have a more directional growth in a certain axis is confirmed with the XRD results, and that ratio has the higher crystallinity as shown in Figure 3.

The EDX spectra (Figure 5) confirmed the semiconductor formation. All the elements that formed the $Bi_2S_{3-x}Se_x$ are present in the EDX spectra. In addition to the constitute elements, there is a peak to carbon which is attributed to the grid that used in measurement and a peak of the Oxygen comes out from aqueous solution during the preparation or processing.

Optical properties

Figure 6 shows the optical absorption spectra of $Bi_2S_{3-x}Se_x$/PMMA nanocomposite films at different compositions x. All samples have a broad absorption character over the entire visible region; this property is required in many applications, including light absorb dependent. According to the Tauc's law [22], the optical band gap can be determined by the equation:

$$\alpha(h\nu) = A\left(h\nu - E_g\right)^n \quad (1)$$

where α(hυ) is the absorption coefficient, E_g is the optical band gap, A is a constant, and n is a parameter that depends on the type of electronic transition which is responsible for the absorption (n = 1/2 for direct transition). The inset in Figure 6 shows that plot of $[\alpha(h\upsilon)]^2$ versus photon energy (hυ).

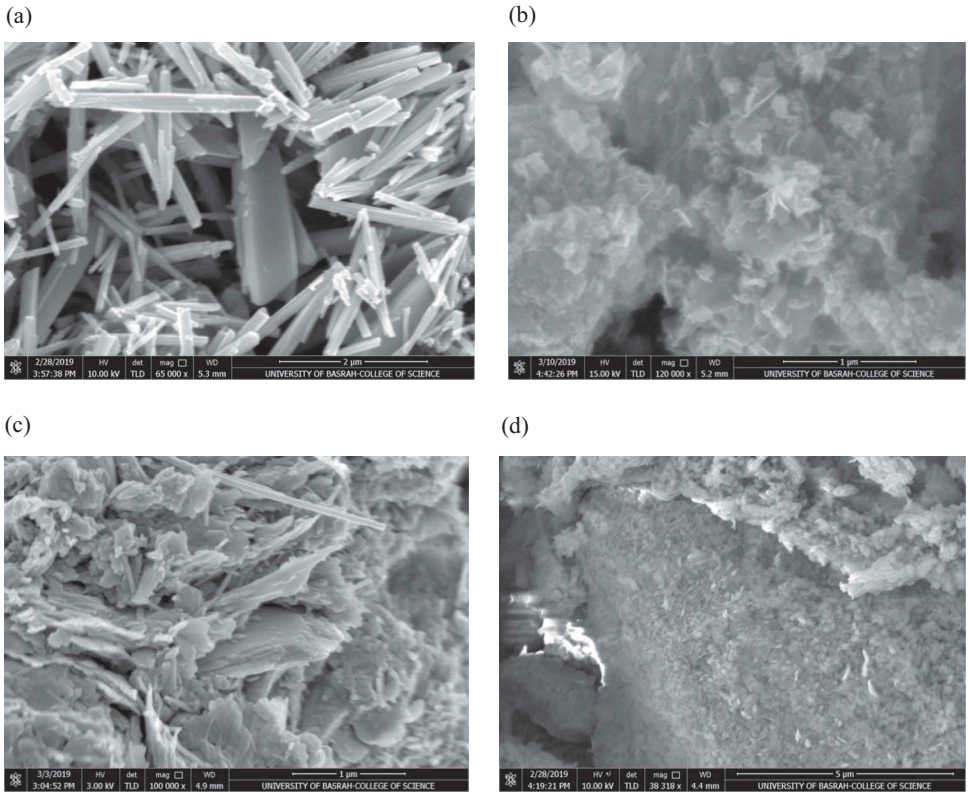

Figure 4. SEM images of $Bi_2S_{3-x}Se_x$/PMMA nanocomposite films at different four compositions, x = 0.0, 0.2, 0.4, and 1.0.

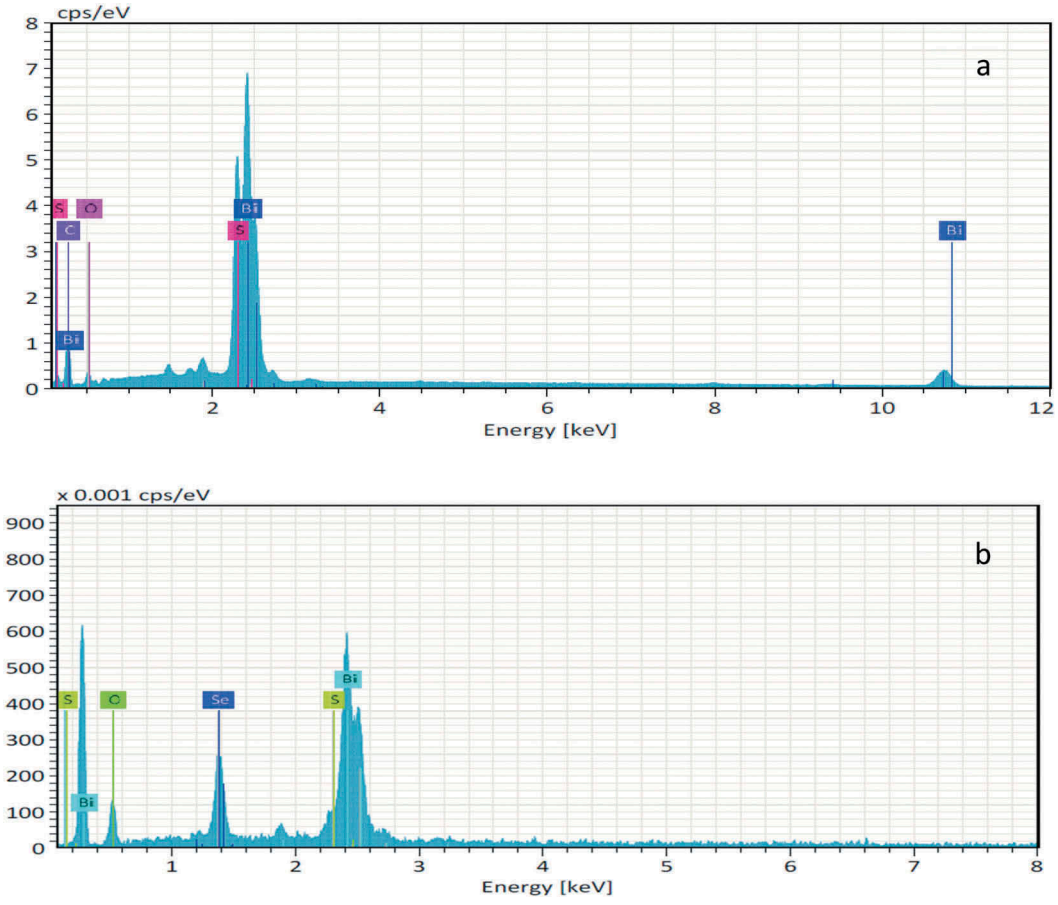

Figure 5. EDX spectrum of $Bi_2S_{3-x}Se_x$/PMMA nanocomposite films for composition (a) x = 0.0 and (b) x = 0.4.

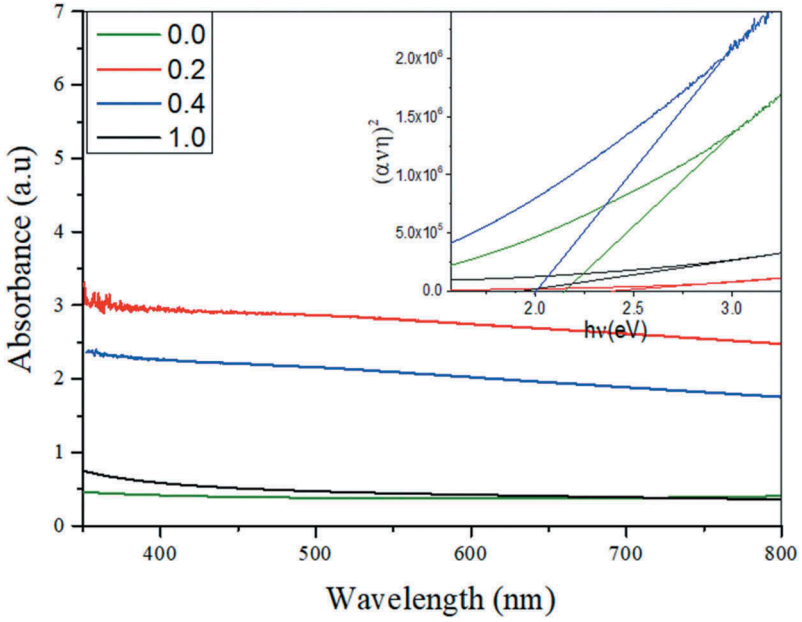

Figure 6. Optical absorption spectra of $Bi_2S_{3-x}Se_x$/PMMA nanocomposite films with different compositions x of 0.0, 0.2, 0.4, and 1.0. The inset is the plot of $(\alpha h\upsilon)^2$ as a function of hυ.

The values of the energy gap of $Bi_2S_{3-x}Se_x$/PMMA nanocomposite films are 2.07, 2.17 and 2.35 eV for x = 0.0, 0.2 and 0.4, respectively. The optical band gap of bulk Bi_2S_3 is 1.3 eV (absorption edge of 946.15 nm) [23]. We observed that the prepared nanocomposite films exhibited a blue shift in the absorption edge for these ratios compared to the absorption edge of bulk Bi_2S_3. When the Se:S ratio is equal to 1.0, the optical band gap decreases to the value of 1.88 eV. This lowering in the optical band gap can be attributed to that of the $Bi_2S_{3-x}Se_x$ which became richer with selenium than sulphur. And because of this, the optical band gap of bismuth selenide is less than from the Bi_2Se_3, which leads to this lowering. This case is similar to other materials [24].

Nonlinear optical response

The nonlinear optical response of the prepared samples was investigated using a modified Z-scan technique as reported in our previous work [25]. Figure 7 shows the nonlinear optical response of $Bi_2S_{3-x}Se_x$/PMMA nanocomposite films with different compositions x = 0.0, 0.2, 0.4, and 1.0. The normalised transmission of nanocomposite samples was measured as a function of sample position (Z) for Z-scan results at varying input powers. The Z-scan data give us information about the nonlinear optical refractive index n_2 and nonlinear absorption β parameters. It can be observed that the variation of these parameters with increasing of composition x leading to the change of the sign of nonlinear refractive index from negative to positive (Figure 7 (I)) and nonlinear absorption from saturable absorption (SA) to reverse absorption (RA), and then to SA with change in Se concentration (Figure 7 (II)).

It is interesting to have in Figure 7 that the behaviours of the nonlinear refraction and nonlinear absorption change in the prepared $Bi_2S_{3-x}Se_x$/PMMA nanocomposite films at different sample compositions from 0.0 up to 1. In the nonlinear refractive regime, the nanocomposite films with compositions of 0.0 and 0.4 exhibit negative refractive index, while the nanocomposite films at 0.2 and 1 composition display positive refractive index. Indeed, the results show that the nanocomposite films changeover in the behaviours related to the response of the input laser beam. That means the NNLR is changed to PNLR and vice versa with n_2 increases with the increase of composition as shown in Table 1. The change in the sign of the nonlinear refractive index behaviour can be interpreted to the fact that as the Se concentration ratio of the excited electrons increases which increases the nonlinear refraction effect in self-focusing, similarly to the case of the other materials [26–28].

In the nonlinear absorption regime, the nanocomposite films correspond to the compositions of 0.0 and 1.0, and the SA gets gradually reinforced. Also, the nanocomposite films prepared with compositions of 0.2 and 0.4, the films were found to be switched to RSA. That means the SA is turned to RSA with β increases with the increase of composition. Then, by increasing the composition x up to 1.0, the film was also switched to SA again with β decreases as shown in Table 1. The change in the nonlinear absorption behaviours can be related to the film absorbing the laser beam and could probably generate enough number of carriers to fill band states up to and including those of the optical transition. Then, the interplay of absorption band leads to bleach. This phenomenon is similar to the case of other materials [26–28].

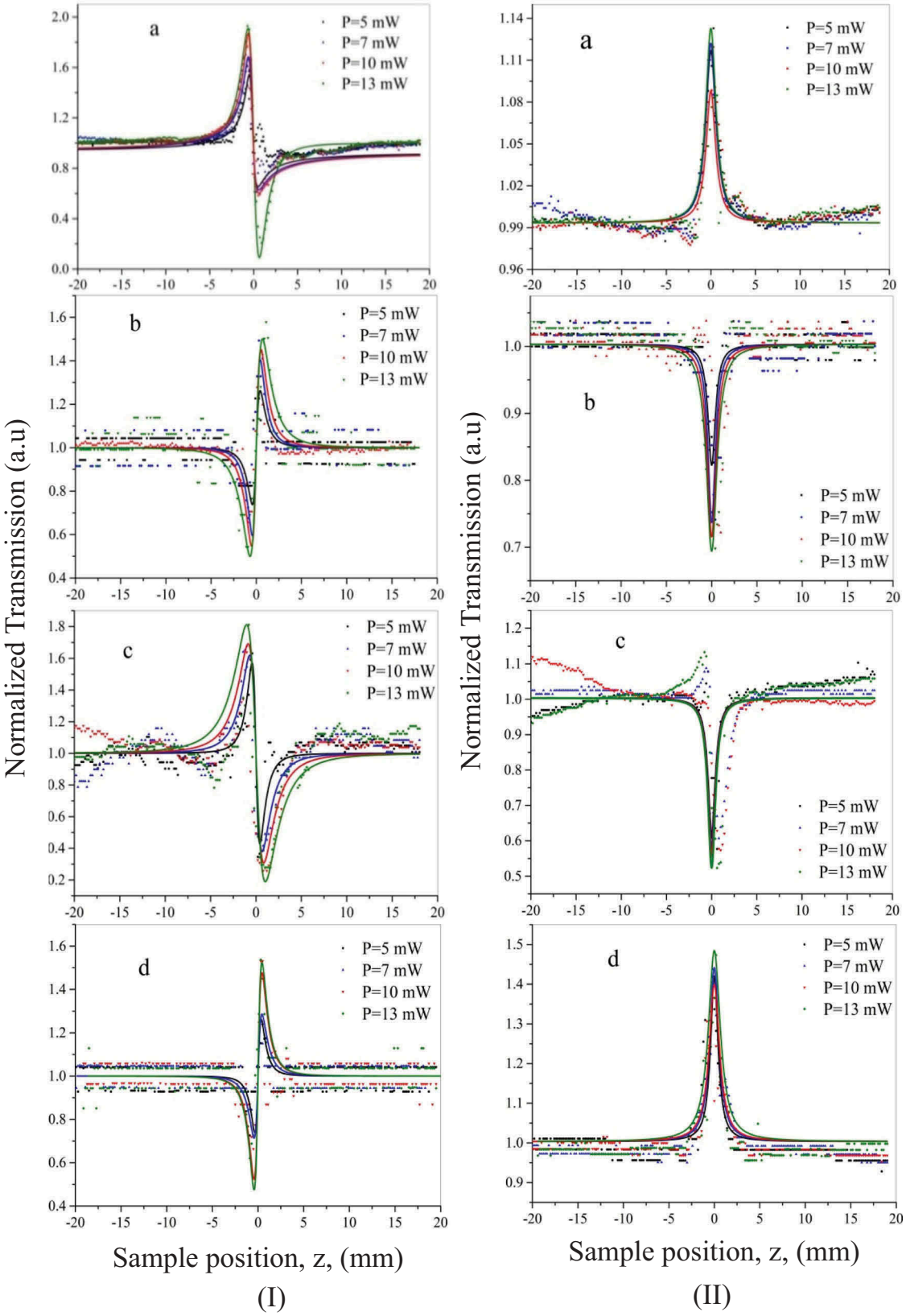

Figure 7. (I) closed-aperture and (II) Open-aperture Z-scan results at different input powers of the $Bi_2S_{3-x}Se_x$/PMMA nanocomposite films with different compositions: (a) 0.0, (b) 0.2, (c) 0.4, and (d) 1.0. The solid lines are theoretical fitting.

From the above results in Figure 7, it can be seen that the nonlinear refraction and absorption response show changeover in the sign of the optical nonlinearity. This can also be attributed generally to that regardless of the polymer matrix or the dispersing agent used and may be the polymer leads to get a dispersed prepared nanocomposite films. In addition, shapes of nanostructures have an important effect on the nonlinear optical behaviours as shown in Figure 4. In addition, the efficient control of nonlinear absorption

Table 1. All-optical switching parameters for the $Bi_2S_{3-x}Se_x$/PMMA nanocomposite films with four different compositions of 0.0, 0.2, and 0.4, and 1.0 at 532 nm laser excitation.

	n_2 x 10^{-10} (m^2/W)				β x 10^{-4} (m/W)				W				T			
	Composition, x				Composition, x				Composition, x				Composition, x			
Input power (mW)	0.0	0.2	0.4	1.0	0.0	0.2	0.4	1.0	0.0	0.2	0.4	1.0	0.0	0.2	0.4	1.0
5	−1.77	8.09	−8.72	11.14	−4.1	12.6	20.5	−5.7	0.93	0.7	3.57	4.5	1.19	0.81	1.2	0.3
7	−1.75	6.1	−6.64	10.5	−3	9.19	16.3	−6.18	0.92	0.5	2.7	4.33	0.75	0.79	1.32	0.31
10	−1.47	6.97	−5.21	7.9	−2.3	7	10	−4.65	0.77	0.6	2	3.2	0.72	0.53	1.1	0.31
13	−1.4	5.79	−3.45	6.98	−1.4	5.6	7.9	−5.42	0.74	0.5	1.4	2.8	0.36	0.51	1.2	0.41

response can lead to the applications in the mode-locking laser and in the protection from laser damage from eyes.

The physical mechanism of the nonlinear refraction in nonlinear optical (NLO) material can be electronic, molecular, and thermal in natural effect [29,30]. In our work, at CW laser, the nanocomposite films are due to thermal effect. The Z-scan curves for all nanocomposite films showed approximately a peak-valley separation of $2Z_0$. If the peak-valley separation is more than 1.7 times the Z_0, it does satisfy the condition for thermal nonlinearity. The nonlinear refractive index n_2 can be given by the following equation [30]:

$$\Delta T_{p-v} = 0.406(1-S)^{0.25}|\Delta\emptyset_0| \tag{2}$$

where S is the linear transmittance of the aperture given by $S = 1 - exp\left(-r_a^2/w_a^2\right)$, w_a is the radius of the laser spot before the aperture, r_a is the radius of the aperture and $\Delta\emptyset_0$ is phase shift given by the relationship [30]:

$$|\Delta\emptyset_0| = kL_{eff}n_2I_0 \tag{3}$$

where ΔT_{p-v} is the peak-valley transmittance difference from the closed aperture z-scan curve, L_{eff} is the effective thickness of the sample given by $L_{eff} = (1 - exp(-\alpha L))/\alpha$, k is the wave vector, I_0 is the intensity of the laser beam at focus and α is the linear adsorption. The normalised transmittance in the case of closed-aperture Z-scan is [30]:

$$T(Z) = 1 - \frac{4x}{(x^2+9)(x^2+1)}\Delta\emptyset_0 \tag{4}$$

where $x = z/z_0$.

In addition, the physical mechanism of the nonlinear absorption can be due to a change in absorption with increasing or decreasing intensity. That mean can be saturable absorption (SA) which leads to the decrease in absorption of light in the material, and reverse saturable absorption (RSA) which leads to the increase in absorption of light in the material [31,32]. RSA and SA can be caused by two-photon absorption (TPA), free carrier absorption (FCA), and nonlinear scattering. When the energy band gap $E_g > 2E_{photon}$, the TPA is the dominant mechanism. In the present work, the results attribute to SA and RSA in the origin of the nanocomposite films. Hence, the TPA is insignificant. The nonlinear absorption β can be given by [30]:

$$\beta = \frac{2\sqrt{2}\Delta T}{L_{eff}I_0} \tag{5}$$

where ΔT is the normalised transmittance. The normalised transmission is given by [30]:

$$T(Z) = \sum\nolimits_{m=0}^{\infty} \frac{[-q_0(Z,0)]^m}{(m+1)^{3/2}} \tag{6}$$

where $q_0 = \frac{\beta I_0 L_{eff} Z_0^2}{Z^2+Z_0^2}$, m is integer.

In practice, for an NLO material to be good in such device, it must have not only large nonlinear refractive index n_2 and small nonlinear absorption coefficient β as can as possible, but also satisfactory 'all- optical figures of merit' [33]. Therefore, the all-optical figures of merit (FOM) are used to evaluate the quality of the NLO material for all-photonic switching devices. Thus, two all-optical figures of merit are defined as [34]:

$$W = \frac{|n_2|I}{\alpha\lambda} \tag{7}$$

and the second one is

$$T = \frac{\beta\lambda}{n_2} \tag{8}$$

In order for an NLO material to be promised for all-optical photonic switching, it is necessary to be $W > 1$ and $T < 1$ [34–36].

To apply all-photonic switching to devices using the prepared nanocomposite films, optimal all-optical figures of merit are needed. The critical threshold Se concentration (composition x) of the film is another important parameter when using this film in all-photonic switching devices. According to Equations (3), (5), (7), and (8) as well using all the measured values of the different optical properties, the obtained values of nonlinear refractive index n_2, nonlinear absorption β, and all-optical figures of merit W and T for the all prepared samples are given in Table 1.

From Table 1, it is observed that with increasing input power of the laser beam, the nonlinear refractive index n_2 increases, which is similar behaviour with the results reported in Tripathi et al. [37]. Also, nonlinear refractive index n_2 decreasing in the order of x composition 0.4 > 0.0 as a self-defocusing effect and 1.0 > 0.2 as a self-focusing effect are seen in the figure. Thus, the sample $Bi_2S_{3-x}Se_x$/PMMA with Se:S ratio or composition of

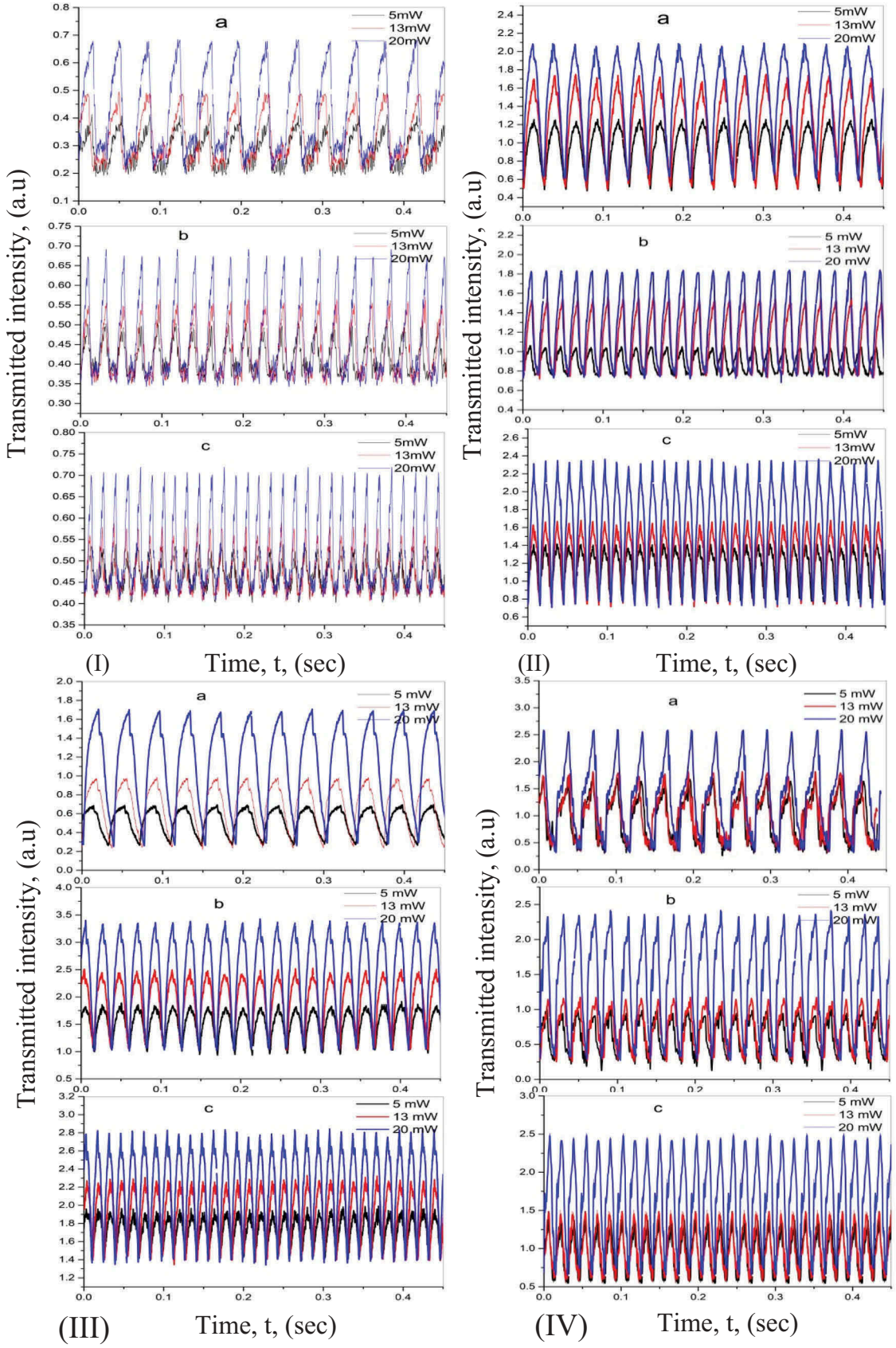

Figure 8. Effect of x composition on all-optical switching of $Bi_2S_{3-x}Se_x$/PMMA nanocomposite films under pump beam powers with different modulation frequencies for x composition (I) 0.0, (II) 0.2, (III) 0.4, and (IV) 1.0: (a) 5 Hz, (b) 10 Hz, and (c) 15 Hz.

x equal to 0.4 has the highest optical nonlinearity compared with the other samples. That could be due to the high crystallinity along with thermal results in large nonlinear optical responses. As mentioned above, the nanowire has a higher crystallinity compared with the nanosheets' morphology (x = 0.2 and 1.0) [38]. For comparison, values of nonlinear optical coefficients n_2 and β of the solution Bi_2S_3 sample reported by other authors at

532 nm laser pulses have been extracted [39,40]. It is shown that these coefficients in our work are less than the others. It may be related to the use of pulse laser at 532 nm that makes the physical mechanism due to electronic instead of thermal in nature under CW laser.

It is also clear that the all-optical figures of merit W appear to be optimised at different input powers with the composition of x = 0.4 and 1.0 for samples exhibited self-defocusing and self-focusing effect, respectively. In contrast, the optimised value for T with the composition of 1.0 and 0.2 for samples exhibited SA and RSA, respectively. Interestingly, the figures of merit are quite useful for practical applications due to the fact that, at that Se concentration, the optical nonlinearity is enhanced and hence the all-figures of merit will be very important to realise all-photonic switching. The enhancement of nonlinearity for these films can be attributed to the changing in E_g of the films with increasing in the Se concentration, and accordingly the absorption coefficient is decreased.

All-optical switching effect

The all-optical switching effect of $Bi_2S_{3-x}Se_x$/PMMA nanocomposite films originates from the propagation of the probe beam, and the latter from the change of nonlinear refractive index of $Bi_2S_{3-x}Se_x$/PMMA nanocomposite films under the excitation of the pump beam. The self-defocusing and self-focusing effect under CW laser associated with thermal nonlinearity origin can be used as an all-photonic switching device. All-optical switching based on nonlinear response was investigated. Figure 8 shows the all-optical switching effects of $Bi_2S_{3-x}Se_x$/PMMA nanocomposite films with different compositions of 0.0, 0.2, 0.4, and 1.0. In this figure, the transmitted intensity as a function of time (t)

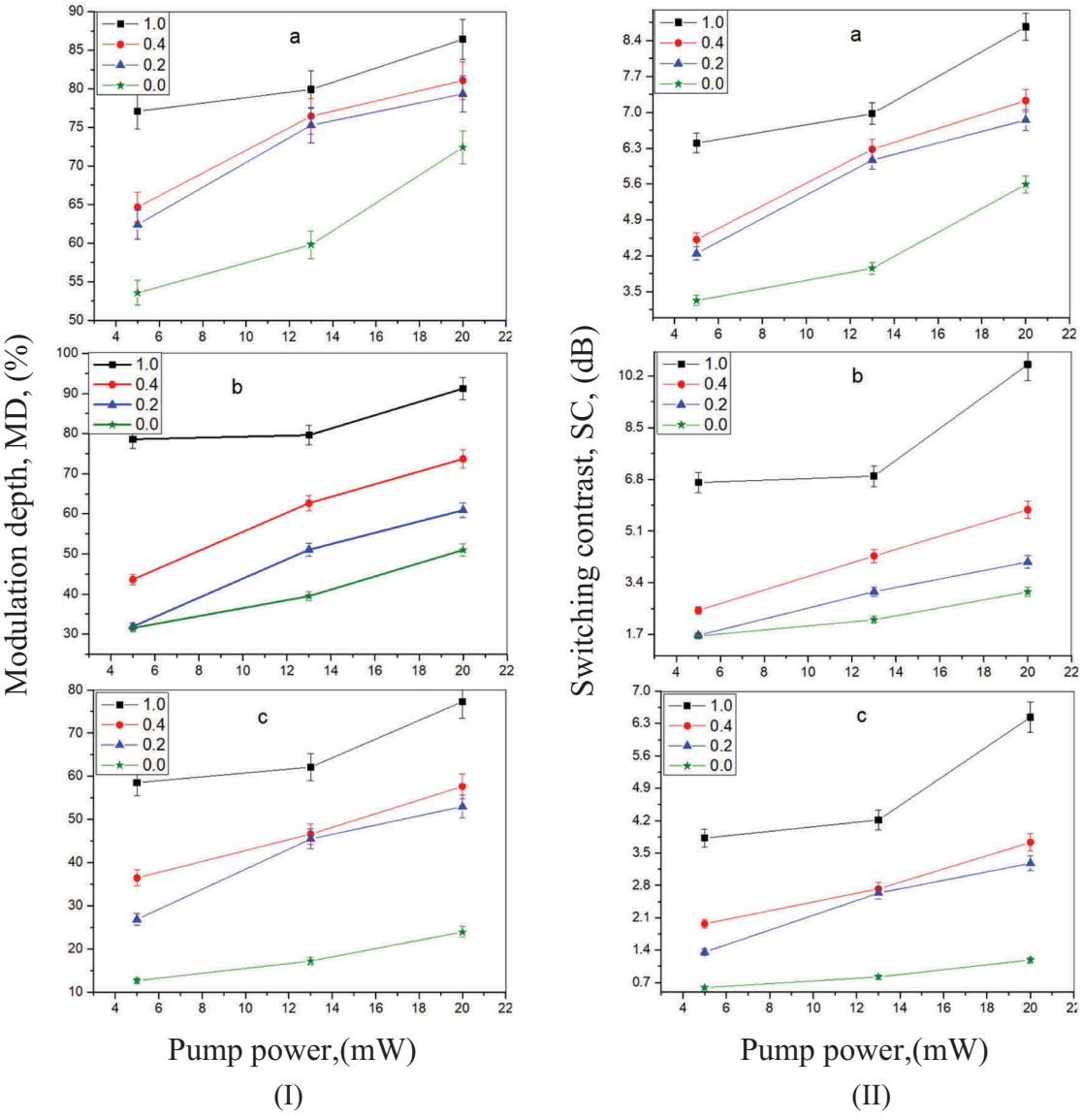

Figure 9. Variation of (I) modulation depth and (II) switching contrast with pump beam powers for $Bi_2S_{3-x}Se_x$/PMMA nanocomposite films with different compositions x: (a) 5 Hz, (b) 10 Hz, and (c) 15 Hz.

was measured at different modulation frequencies (f_m) of 5, 10, and 15 Hz, and input pump powers (P_p) of 5, 13, and 20 mW. It is noted that at 5 Hz modulation frequency and different pump powers in the whole time range, the nanocomposite film with compositions of 0.4 and 1.0 for samples exhibited self-defocusing and self-focusing effect, respectively, had the highest all-optical switching effects in the output, i.e. the nonlinear refractive index of $Bi_2S_{3-x}Se_x$/PMMA nanocomposite films is the largest in the compositions of 0.4 and 1.0. This can be attributed to the higher figures of merit which led to the strongest photoinduced anisotropy (see Table 1).

Parameters of all-photonic switching

To achieve good all-optical switching, some important information such as low input pump power, high SC, large MD, and fast ST are required [10,41]. The critical threshold Se:S ratio concentration or x composition of the nanocomposite film is another important parameter when using this material in this device. The variations in MD and SC as a function of Pp at three different f_m were studied. The results are illustrated in Figure 9 for the $Bi_2S_{3-x}Se_x$/PMMA nanocomposite films with four compositions of 0.0, 0.2, 0.4, and 1.0. It is clear that when the x composition of the nanocomposite films increases, the MD and SC increased at the same modulation frequency. However, increasing the modulation frequency led to decreased MD and SC. This is because, at higher frequency, the electrons did not have enough time to return to the equilibrium state.

The switching time ST is another important parameter for all-optical photonic switching. Figure 10 shows the modulation frequency dispersion of ST for all the prepared $Bi_2S_{3-x}Se_x$/PMMA nanocomposite films using various compositions under pump beam powers 5, 13, and 20 mW. The ST decreased with increasing modulation frequency and pump powers, which leads to fast response time for the composition of 0.4 and 1.0 for samples exhibited self-defocusing and self-focusing behaviours.

From the obtained results, it is shown that the all-optical switching with high MD and SC can be obtained with low pump and probe beam power as soon as possible. Consequently, in spite of its higher MD and SC, the $Bi_2S_{3-x}Se_x$/PMMA nanocomposite film at x composition of 0.4 and 1.0, respectively, ensures for all-optical switching device in all-optical communication systems a much smaller value of ST equal to 14 and 13 ms, hence much higher values of MD = 76% and 80% and SC = 6.2 dB and 7 dB compared with other samples.

Conclusion

We have built a two-colour optical pump-probe technique by pumping the material simultaneously, which

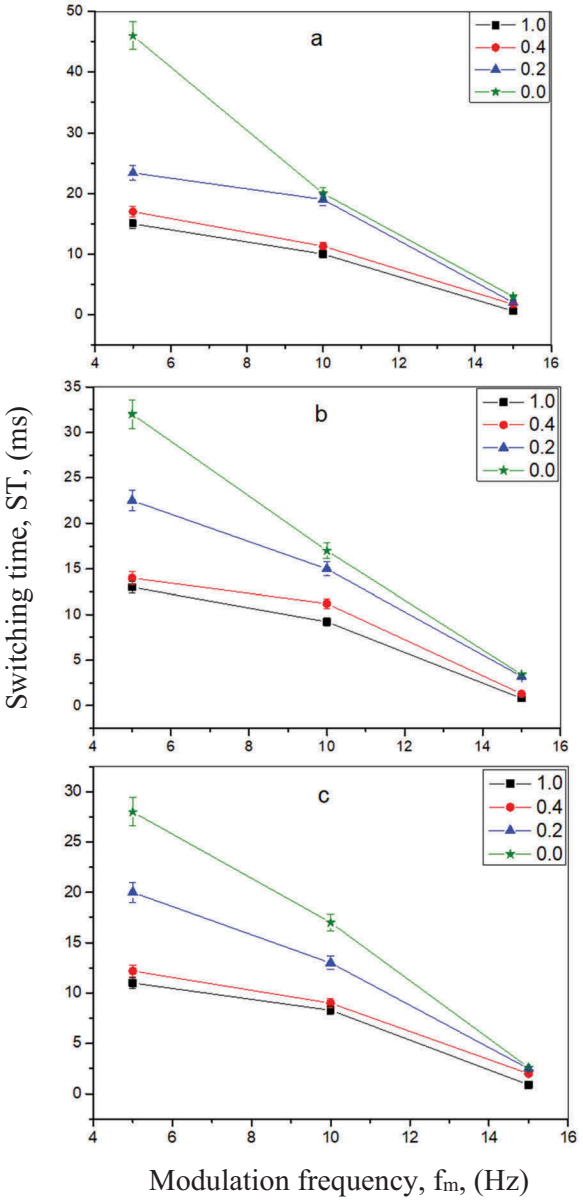

Figure 10. Switching time with modulation frequency under different pump powers for $Bi_2S_{3-x}Se_x$/PMMA nanocomposite films with different compositions x.

is capable of measuring the MD, SC, and ST at a certain value of input pump laser power.

$Bi_2S_{3-x}Se_x$/PMMA under various x compositions of 0.0, 0.2, 0.4, 1.0 were prepared using a microwave-assisted synthesis. The nonlinear optical response of thermal origin exhibited by the $Bi_2S_{3-x}Se_x$/PMMA nanocomposite films using various x compositions at input laser powers was studied and all-optical switching effect based on nonlinear response is investigated. The nonlinear response was determined by the z-scan technique and analysed on the basis of thermal in nature and SA and RSA in origin corresponding to the nonlinear refractive index and nonlinear absorption, respectively. The variation in the output intensity was studied as a function of input laser power. Fast nonlinear response and optimised values of the all-optical figures of merit for all-optical photonic switching were

obtained by adjusting the x composition and the input pump power. The results obtained all-optical figures of merit due to the best crystalline nature of compositions of 0.4 and 1.0 among all other samples.

The present results will be useful for the design of all-optical photonic switching device at the threshold pump power of 13 mW in the modulation frequency of 5 Hz. The device was prepared using $Bi_2S_{3-x}Se_x$ /PMMA by the composition of 0.3 at MD of 76% and SC of 6.2 dB at ST of 14 ms, and composition of 1.0 at MD of 80% and SC of 7dB at ST of 13 ms.

Disclosure statement

No potential conflict of interest was reported by the authors.

References

[1] Clark J, Lanzani G. Organic photonics for communications. Nat Photonics. 2010;4:438.

[2] Hu XY, Jiang P, Ding CY, et al. Picosecond and low-power all-optical switching based on an organic photonic-bandgap microcavity. Nat Photonics. 2008;2:185–189.

[3] Biberman A, Bergman K. Optical interconnection networks for high-performance computing systems. Rep Prog Phys. 2012;75:046402.

[4] Aspuru-Guzik A, Walther P. Photonic quantum simulators. Nat Phys. 2012;8:285–291.

[5] Kumar P, Mathpal MC, Hamad S, et al. Cu nanoclusters in ion exchanged soda-lime glass: study of SPR and nonlinear optical behavior for photonics. Appl Mater Today. 2019;15:323–334.

[6] Anand B, Podila R, Lingam K, et al. Optical diode action from axially asymmetric nonlinearity in an all-carbon solid-state device. Nano Lett. 2013;13:5771–5776.

[7] Pezeshki H, Ahmadi V. All-optical bistable switching based on photonic crystal slab nanocavity using nonlinear Kerr effect. J Mod Opt. 2013;60:103–108.

[8] Rahma MA, Saadon HL, Mahdi MA. All-photonic switching based on selective input pump polarization states in Fe-doped PbS/PVA freestanding nanocomposite films. J Phys D: Appl Phys. 2017;50:135103.

[9] Dong Y, Deepika Saini LA, Echegoyen RP. Passive optical switches based on endohedral fullerenes. Opt Mater. 2016;53:14–18.

[10] Qin F, Liu Y, Meng ZM, et al. Design of kerr- effect sensitive microcavity in nonlinear photonic crystal slabs for all-optical switching. J Appl Phys. 2010;108:053108.

[11] Reyna AS, de Araújo CB. An optimization procedure for the design of all-optical switches based on metal-dielectric nanocomposites. Opt Express. 2015;23:7659–7666.

[12] (a) Song Y, Chen Y, Jiang X, et al. Nonlinear few-layer antimonene-based all-optical signal processing: ultrafast optical switching and high-speed wavelength conversion. Adv Opt Mater. 2018;6:1701287.

[13] Zheng J, Tang X, Yang Z, et al. Few-layer phosphorene-decorated microfiber for all-optical thresholding and optical modulation. Adv Optical Mater. 2017;5:1700026.

[14] Wang K, Zheng J, Huang H, et al. All-optical signal processing in few-layer bismuthene coated microfiber: towards applications in optical fiber systems. Opt Express. 2019;27:16798–16810.

[15] Kumar A, Punia R, Gupta AK, et al. Study of all-optical switching properties of zinc phthalocyanine thin film by pump-probe technique. Opt Laser Technol. 2017;95:100–104.

[16] Oya M, Kishikawa H, Goto N, et al. All- optical switch consisting of two-stage interferometers controlled by using saturable absorption of monolayer graphene. Opt Express. 2012;20:27322–27330.

[17] Hu X, Jiang P, Xin C, et al. Nano- Ag:polymeric composite material for ultrafast photonic crystal all- optical switching. Appl Phys Lett. 2009;94:031103/1–4.

[18] Tao S, Miyagoe T, Maeda A, et al. Ultrafast optical switching by using nanocrystals of a halogen-bridged nickel-chain compound dispersed in an optical polymer. Adv Mater. 2007;19:2707–2710.

[19] ASTEM Powder Data File, JCPDS 170320 Card

[20] Adam A, El-Khouly A, Lilov E, et al. Ultra thin bismuth selenide-bismuth telluride layers for thermoelectric applications. Mater Chem Phys. 2019;224:264–270.

[21] Kumari V, Kumar V, Malik BP, et al. Nonlinear optical properties of erbium doped zinc oxide (EZO) thin films. Opt Commun. 2012;285:2182–2188.

[22] Kondyurin A, Bilek M. Beam treatment of polymers: application aspects from medicine to space. Amsterdam: Elsevier; 2008.

[23] He R, Qian XF, Yin J, et al. Preparation of Bi2S3 nanowhiskers and their morphologies. J Cryst Growth. 2003;252:505–510.

[24] Hsynes WM. Handbook of chemistry and physics. 97th ed. CRC Press: Taylor Francis Group; 2016.

[25] Rahma MA, Saadon HL, Mahdi MA. High-performance all-optical limiting based on nonlinear refraction of metal-doped PbS/PVA freestanding nanocomposite films films. Optik. 2018;174:580–590.

[26] Demetrios Christodoulides N, Choon Khoo I, Salamo GJ, et al. Nonlinear refraction and absorption: mechanisms and magnitudes. Adv Opt Photonics. 2010;2:60–200.

[27] Almosawe A, Saadon HL. Nonlinear optical and optical limiting properties of new structures of organic nonlinear optical materials for photonic applications. Chi Opt Lett. 2013;11:041902–041905.

[28] Quan C, He M, He C, et al. Transition from saturable absorption to reverse saturable absorption in MoTe2 nano-films with thickness and pump intensity. Appl Surf Sci. 2018;457:115–120.

[29] Saadon HL. Z-scan studies and optical limiting in a new organic-polymer composite film. Opt Quantum Electron. 2016;40:1–8.

[30] Sheik-Bahae M, Said AA, Wei TH, et al. Sensitive measurement of optical nonlinearities using a single beam. IEEE J Quantum Electron. 1990;26:760–769.

[31] Naga Srinivas NKM, Venugopal Rao S, Narayana Rao D. Saturable and reverse saturable absorption of Rhodamine B in methanol and water. J Opt Soc Am B. 2003;20:2470.

[32] Kurum U, Yuksek M, Yagliolu HG, et al. The effect of thickness and/or doping on the nonlinear and saturable absorption behaviors in amorphous GaSe thin films. J Appl Phys. 2010;108:063102.

[33] Tian T, Fang Z, Shuizhu W, et al. Photo-induced birefringence and all-optical switching effect in azobenzene-grafted polyurethanes. Opt Mater. 2004;27:585–590.

[34] Stegeman GI. Material figures of merit and implications to all- optical waveguide switching. SPIE Proc. 1993;1852:75–89.
[35] Lin Y, Zhang J, Brzozowski L, et al. Nonlinear optical figures of merit of processible composite of poly.2-methoxy,5-.28-.ethyl.hexyloxy.-p-phenylene vinylene. And poly.methyl methacrylate. J Appl Phys. 2002;91:522–524.
[36] Huang T, Hao Z, Gong H, et al. Third-order nonlinear optical properties of a new copper coordination compound: A promising candidate for all- optical switching. Chem Phys Lett. 2008;451:213–217.
[37] Tripathi SK, Ramneek K, Yoti J. Investigation of nonlinear optical properties of CdS/PS polymer nanocomposite synthesized by chemical route. Opt Commun. 2015;352:55–62.
[38] Shuguang C, Xueqing X, Xiaoyun Y, et al. Nonlinear optical and optical limiting properties of ultra-long gold nanowires. Mater Lett. 2016;166:51–54.
[39] Lia C, Shia G, Song Y, et al. Third-order nonlinear optical properties of Bi2S3 and Sb2S3 nanorods studied by the Z-scan technique. J Phys Chem Solids. 2008;69:1829–1834.
[40] Chen JLT, Nala V, Kannaiyan G, et al. Synthesis and nonlinear optical switching of Bi2S3 nanorods and enhancement in the NLO response of Bi2S3@Au nanorod-composites. New J Chem. 2014;38:985–992.
[41] Yong Z, Danping L, Cheng Z, et al. Low power and large modulation depth optical bistability in an si photonic crystal L3 cavity. IEEE Photon Technol Lett. 2014;26:2399–2402.